Research Journal of Recent Sciences _____ ISSN 2277-2502
Vol. **1(10),** 37-44, October **(2012)** *Res.J.Recent Sci.*

Uniaxial Growth and Characterization studies of [(para methoxy phenyl) imino] benzene NLO crystal by Sankaranarayanan- Ramasamy Method

Anbarasu S. and Devarajan Prem Anand
Department of Physics, St. Xavier's College (Autonomous), Palayamkottai – 627002, INDIA

Available online at: www.isca.in
Received 24th July 2012, revised 8th August 2012, accepted 10th August 2012

Abstract

Optically transparent bulk single crystal of [(para methoxy) phenyl] imino benzene (PMPIB) has been grown along <013> plane using the uniaxial crystal growth method of Sankaranarayanan-Ramasamy with a new modification in the growth assembly. The crystal was grown with a growth rate of 6mm/day upto a dimension of 60 X 30 X 10 mm and within a period of 10 days having a cylindrical morphology. Single crystal XRD analysis confirms that the growth ingot belongs to the orthorhombic crystal system with a space group of P_{212121}. The crystalline perfection was assessed by XRPD analysis. The powder diffraction pattern of the grown crystal has been indexed. The presence of C=N bond with intramolecular hydrogen bonding on the protonation of ions were confirmed by FTIR analysis. The UV-vis-NIR spectrum of the crystal shows that the crystal has cut-off wavelength at 200 nm. The $_1H^1$ and ^{13} NMR spectra confirms the molecular structure. The existence of second harmonic generation (SHG) signal was observed by using ND:YAG laser with the fundamental wavelength of 1064 nm. The Laser damage threshold of PMPIB was found to be 0.57 GW/cm^2 and hence PMPIB can be used in frequency doubler system. The photoconductivity study of PMPIB revealed negative photoconductivity of the sample.

Key-words: PMPIB, S-R method, XRPD, FTIR, UV-vis-NIR, NMR

Introduction

A major effort was developed to use the nonlinear optical (NLO) effect in materials to generate frequencies that are not available and also to develop the capacity of generating tunable coherent beams[1-4]. Much of the research has been directed towards materials that produce second harmonic generation, the frequency doubling of laser light, telecommunication, optical computing, optical data storage and optical information processing[5-6]. To realize the consumption, it is necessary to have highly polarizable molecules aligned in a head to tail fashion, connected through hydrogen bond interaction crystallizing in non-centro symmetric structure for an efficient of a second harmonic generation[7]. In view of the above requirements, it is mandatory to search for new organic NLO crystals which possesses short cut-off wavelength, optical quality sufficiently large nonlinear coefficient, transparency in UV region, High damage threshold, higher resistance to optical damage and maneuverability for device applications etc. Recently the second order nonlinear optical property of two anil derivatives and in particular the variations upon switching between the enol-imine and keto-amine forms were investigated by Aurelie Plaquet et al[8]. The molecular modeling and evaluation of NLO activity of two series of imine derivatives of diamino maleonitrile were reported by Volodymyr V. Nesterov et al[9-14]. The experimental and theoretical investigation of an organic active nonlinear optical material N-(4-hydroxy-phenyl)-2-hydroxybenzaldehyde-imine and thiazolo(3, 2-a) pyrimidine derivatives were reported by Yufeng Wang et al[15] and Jotani Mukesh M et al[16] respectively. Several heterocyclic imine derivatives were designed with a general structure D-π-A(D'). Introduction of donor amino group into the absorber moiety were expected to bring H-bonds into the crystal structures and six heterocyclic containing compounds of the type were prepared. Single crystals were grown for five of them and these crystals were characterized by XRD analysis and out of these three compounds namely $C_{10}H_8N_4S$, $C_9H_6N_4O.0.5\ H_2O$ and $C_{13}H_9N_5$ were also found to crystallize in acentric space group thus exhibiting high second order nonlinear optical activity[17]. 4-N-t-butyl-5- arylimino-1,2,4-triazole-3-thione and 5-arylimino-1,2,4-triazolidine-3-thione were synthesized by Rashidi N.A. et al[18]. Prajapathi Ajaypal et al have synthesized some indole derivatives, 2-(substituted aryl)-3-(N'-5-nitro indole acetamiddyl) -4-oxo-thiazolidines[19]. Yaddanapudi Prabhakar carried out solvent free microwave assisted synthesis[20] to prepare 3-(4-Ethylbenzyl)-1- (4-methoxybenzyl)-6-(methylthio)-1, 3, 5-triazine-2,4 (1H, 3H)-dione derivatives. Schiff base ligands as 4-hydroxy-3-(1-(arylimino) ethyl) chromen-2- one were synthesized by Girgaonkar M.V et al [21].

In this report we present our findings of our endeavour on the synthesis, growth and characterization studies of PMPIB by modified Sankaranarayanan-Ramasamy method. The as grown <110> face of the crystal were characterized by single crystal XRD, FTIR, UV-vis-NIR, $_1H^1$ and C_{13} NMR spectral analysis, NLO test, LDTA, Photoconductivity studies so as to improvise the material for blue-green laser radiation.

Material and Methods

All the reagents and solvents were analytical grade (E-Merck) and were used without any further purification. Methoxy benzaldehyde (E-merk) and aniline (E-merk) were commercially available.

Synthesis of PMPIB: The starting material as methoxy benzaldehyde was dissolved in aniline solution in equimolar ratio at a temperature of 30 ^{o}C. The PMPIB was formed in the form of crystalline salt. The crystalline salt was recrystallised thrice using aniline. The as obtained crystalline salt was used for solubility and growth experiments. The reaction scheme is shown in figure 1.

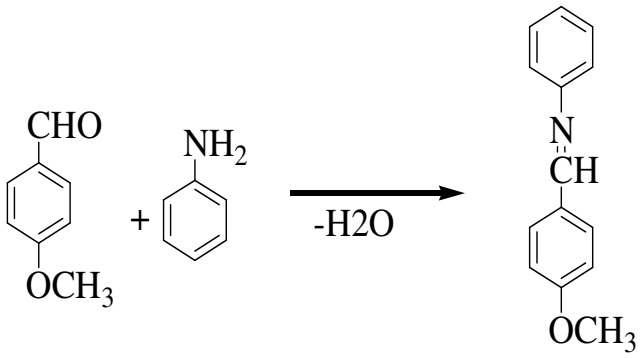

Figure-1
Reaction scheme of PMPIB

Solubility studies of PMPIB: The synthesized salt was used to measure the solubility of pure PMPIB crystals in dimethyl formamide (DMF). A 250 ml borosil glass beaker filled with 100 ml DMF was placed inside a constant temperature bath. An acrylic sheet with a circular hole at the middle was placed over the beaker through which a spindle from an electric motor, placed on the top of the sheet was introduced into the solution. A Teflon paddle was attached at the end of the rod for stirring the solution. The synthesized salt was added in small amounts with DMF solvent and stirring was continued till the formation of precipitate, which confirmed the supersaturation of the solution. A 20 ml of the saturated solution was withdrawn by means of a warmed pipette and the same was poured into a clean, dry and weighed petri dish. The solution was kept in a heating mantle for slow evaporation till the whole of the solution got evaporated and the mass of PMPIB in 20 ml of solution was determined by weighing petri dish with salt and hence the solubility, i.e. quantity of PMPIB salt in gram dissolved in 100 ml of the solvent was determined. The solubility of PMPIB crystals in DMF solvent was determined for five different temperatures (30, 35, 40, 45 and 50 ^{o}C) by adopting the same procedure. The resulting solubility curve of pure PMPIB is shown in figure 2.

Growth Rate of PMPIB: It is well known that the evaporation rate of the solvent dimethyl farmamide (DMF) into the atmosphere is a function of temperature, humidity and air velocity. It is evident that the evaporation process in the atmosphere is diffusion of DMF molecules coming out of its surface through the air larger covering its surface. To calculate theoretically the absolute evaporation rate, we must know the diffusion coefficient of DMF vapour in air and the thickness of the boundary layer accurately. Kazuo Histake et al reported a detailed survey on the evaporation rate[22]. A reaction for the growth rate of SR method is given by R_T = 0.318 K (SE)/r^2d (cm per day), where K is the proportionality constant, S is the solubility of the material (g/ml) of the solvent, E is the evaporation rate of the solvent (ml per day), r is the radius of the vessel, d is the density of the material (g/cm^3) and T is the temperature (K). By using the above parameters, the growth rate of the crystal is calculated. The evaporation rate of the solvent in an ampoule was also measured by observing the lowering rate of the top surface of the solution level.

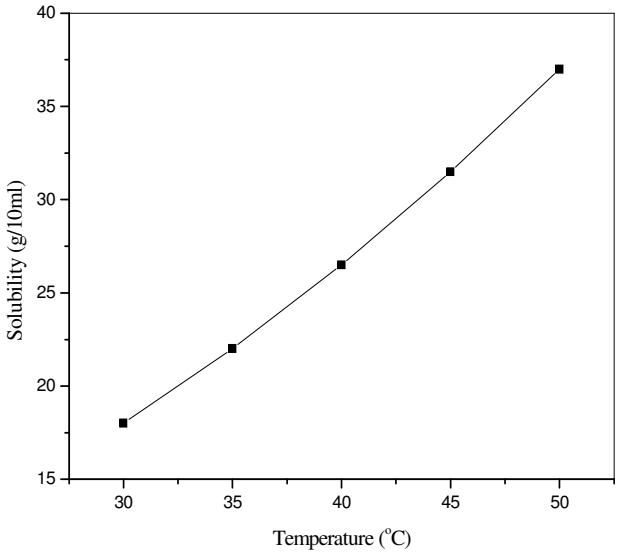

Figure-2
Solubility Curve of PMPIB single crystal

Experimental set-up – S-R method: The experimental set-up for the grown PMPIB single crystal by Sankaranarayanan-Ramasamy method is shown in figure 3. It consists of a growth ampoule made out of glass. A outer glass shield tube protects and holds the inner growth ampoule. Ring heaters were positioned at the top and the bottom of the ampoule which was connected to a temperature controller. The temperature controller provided the necessary temperature for solvent evaporation. The PMPIB solution of optimized saturation was prepared using DMF solvent. The as grown PMPIB single crystal by slow evaporation technique and <013> crystals of PMPIB grown by S-R method are shown in figure 4 and 5 respectively.

Figure-3
Sankaranarayanan-Ramasamy method

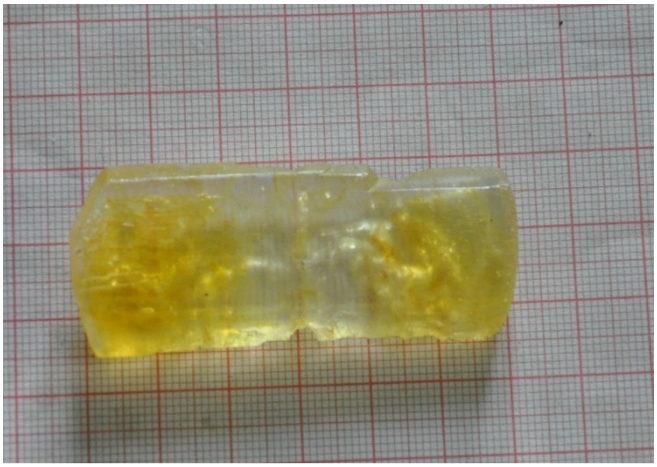

Figure-4
Photograph of as grown crystal of PMPIB by slow evaporation method

Figure-5
Photograph of as grown PMPIB single crystal by S-R method

Results and Discussion

Single Crystal XRD: Single crystal XRD data of the as grown <013> face of PMPIB crystal were obtained using a single crystal X-ray diffractometer (model; Brucker-Nonius K appa Apex II CCD). The PMPIB crystal retained its orthorhombic structure with lattice parameters a= 7.64 Å, b= 12.196 Å, c= 12.254 Å and α= 90°, β= 90°, γ= 90° and V= 1139 Å^3 with non-centro symmetric group P_{212121}.

XRPD analysis: The powder sample of PMPIB crystal was subjected to powder X-ray diffraction studies with Riech Single X-ray diffractometer using CuKα radiation of wavelength λ = 1.5418 Å with a scan speed of 0.2°/sec. The peaks observed from X-ray diffraction spectrum were analyzed and indexed using the proszki software package. Figure 6 shows the XRPD spectrum of PMPIB crystal. The lattice parameter values of PMPIB taken from the single crystal XRD were used for the simulation of hkl values. The data obtained by the XRPD analysis are in accordance with the single crystal XRD data thereby confirming PMPIB belongs to orthorhombic system. It is clear from the XRPD pattern that the PMPIB crystal remains the same with a small change in the intensity level of the peaks. In addition to that the diffracting (hkl) planes also satisfy the general reflection conditions of space group observed from the structure determination of the crystal. The XRPD spectrum ascertains that the environment of the crystal may be affected due to the impurities that might have entered in the crystal lattice occupying only the interstitial positions but not the lattice structure.

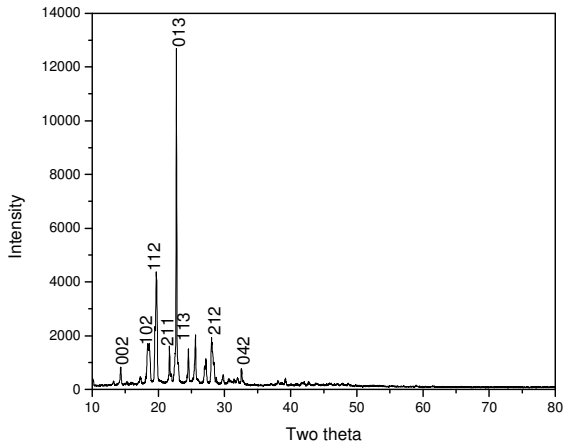

Figure-6
XRPD spectrum of PMPIB single crystal

FTIR analysis: Crystal powders of the pure crystal PMPIB was mixed with KBr in the ratio of 1:10 and palletized using a hydraulic press and subjected to Fourier Transform Infra Red (FTIR) spectroscopic analysis. In order to analyze qualitatively in the presence of various functional groups in PMPIB crystal, The FTIR spectrum was recorded in the range 400-4000 cm^{-1}

employing Brukker model IFS 66V FTIR spectrometer. The IR spectrum of PMPIB is shown in figure 7. The recorded FTIR spectrum was compared with the standard spectra of the functional groups [23-24]. The FTIR spectrum of the compound shows to prominent peaks at 3050 cm^{-1} and 3009 cm^{-1} which corresponds to aromatic C-H stretching. The sharp peaks centered around 2978 $cm^{-1}$and 2937 cm^{-1} are attributed to aliphatic $–CH_3$ stretching. The C=C ring spectra was observed at 1601 cm^{-1} and 1508 cm^{-1}. The appearance of peak at 1248 cm^{-1} is due to the presence of asymmetric C-O-C stretching. The significant appearance of the peak at 1073 cm^{-1} is due to symmetric C-O-C stretching. The aromatic C-N stretching is centered around at 1368 cm^{-1}. A peak at 843 cm^{-1} is due to C-H bending. The absorption band assignable to the stretching of C=N bond was observed at frequency of 1644 cm^{-1}. Thus the FTIR spectra confirm the presence of functional groups and their mode of vibrations.

UV-vis-NIR studies: The UV-visible study of the grown crystal was carried out by Varian Carry 5E spectrometer. The absorption spectrum (figure 8) shows the grown crystal has lower cut-off wavelength around 283 nm. Near UV region, absorption arises from electronic transition associated within the PMPIB moiety. The orbital π- electron delocalization in the molecule may be due to the mesomeric effect. This π- electron dislocation is responsible for its nonlinear optical response and absorption in near UV-region[25]. From the UV-visibbe data, we have plotted a graph of absorption verses photon energy in eV and from the graph, it can be said that band gap is direct type[26]. Thus the grown crystal has a good transmission in UV as well as in visible region. The wide range of transparency of the grown crystal is an added advantage in the field of electronics applications[27].

$_1H^1$ and C^{13} NMR Studies: $_1H^1$ NMR spectrum of PMPIB is shown in figure 9. The powder sample of PMPIB was dissolved in dieurated water with $CDCl_3$ as internal standard. The spectrum was recorded using a Brukker ARX 300 spectrometer in $CDCl_3$ at 23 ^oC. The chemical shift values of the proton were plotted and the $_1H^1$ NMR spectrum of the compound shows a singlet at 3.89 ppm which corresponds to the 3H of the methyl group. The resonance at 8.41 ppm is assignable to a proton of the imine carbon. The multiplets surrounded at 7-7.89 ppm are attributed to aromatic protons. Since the spectrum has no other peaks, the crystal was recorded as a pure. The structure of the compound was further supported by C^{13} NMR spectrum as shown in figure 10. The signal at 55.45 ppm corresponds to the carbon of the methoxy group. The resonance at 159.77 ppm is pertained to the carbon of the benzene ring with the methoxy group substituted. Additionally the signals rising at 110-132 ppm are due to the aromatic ring carbons. The peak at 162 ppm is ascertained to the carbon of the imine moiety. Thus the molecular structure is confirmed by $_1H^1$ and C^{13} NMR spectral analysis.

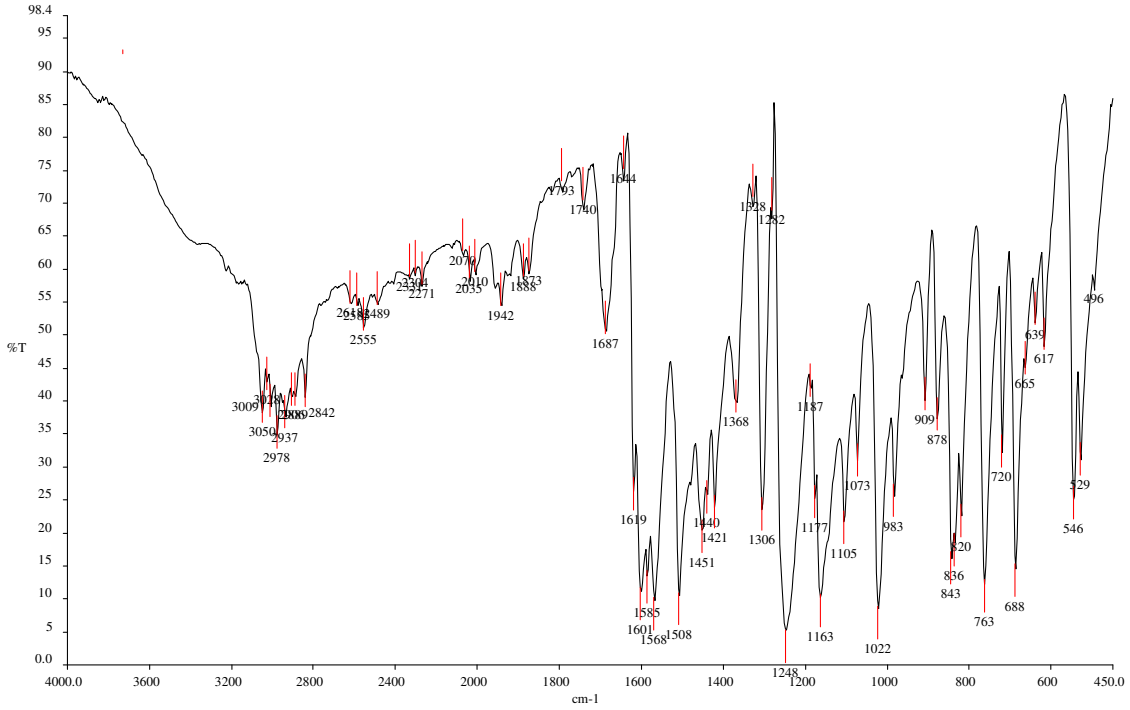

Figure-7
FTIR Spectrum of PMPIB single crystal

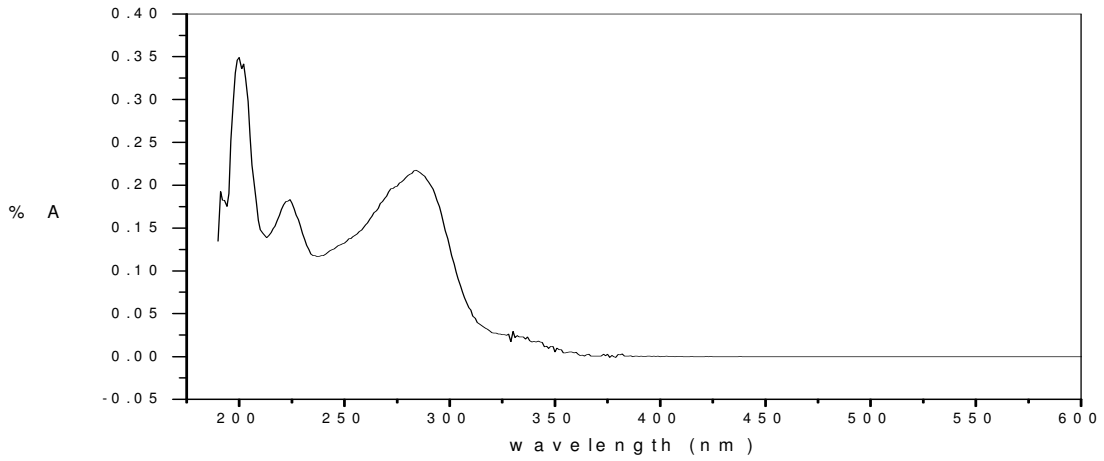

Figure- 8
UV-vis-NIR Spectrum of PMPIB single crystal

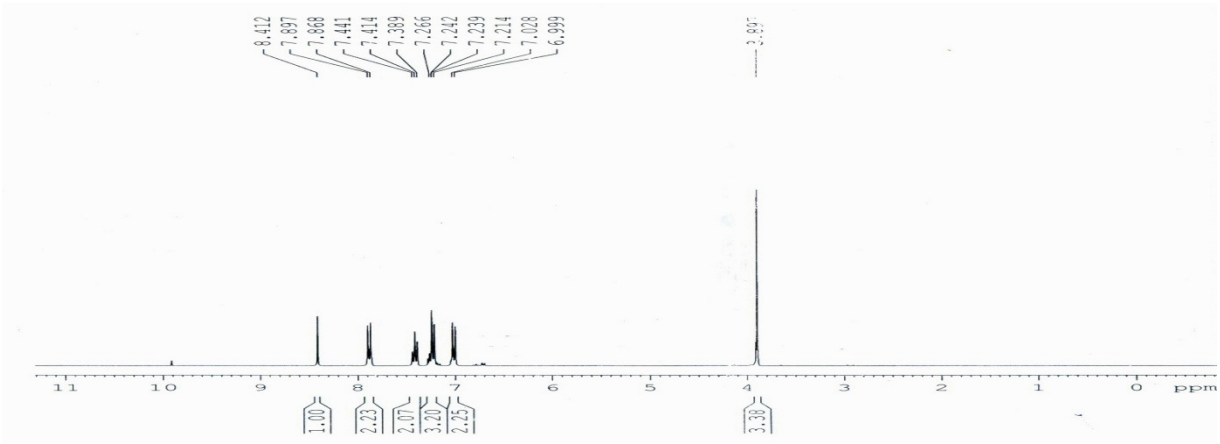

Figure- 9
$_1H^1$ NMR spectrum of PMPIB crystal

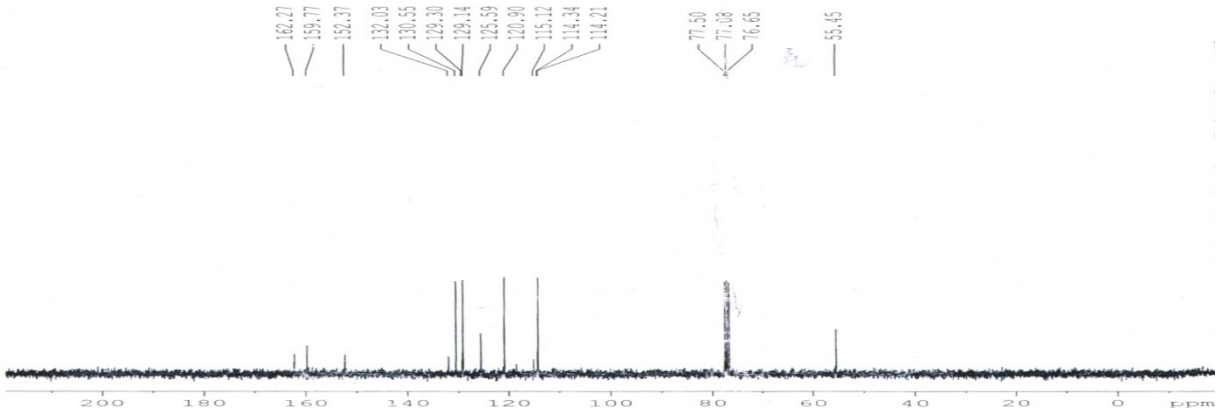

Figure-10
C^{13} NMR spectrum of PMPIB crystal

Photoconductivity Studies: The photoconductivity studies of the PMPIB single crystals were carried out using Keithley 480 picometer. In the absence of any radiation on the sample and by varying the applied field from 20-240 V/cm, the corresponding dark current values were recorded by the picometer. To measure the photocurrent, the sample was illuminated with a halogen lamp (100 W) containing iodine vapor, by focusing a spot of light on the sample with the help of a convex lens. The applied voltage was increased from 20 to 240 V and the corresponding photocurrent was recorded. Photocurrent and dark current were plotted as a function of the applied field as shown in figure 11. It is observed from the plot that dark current is greater than the photocurrent, thus suggesting that PMPIB exhibits negative photoconductivity. The negative photoconductivity exhibited by the sample may be due to the reduction in the number of charge carriers or their life time in the presence of radiation [28-29]. The decrease in lifetime with illumination could be due to the trapping process and increase in carrier velocity given by the relation

$T = (vsN)^{-1}$

Where v is the thermal velocity of the carrier, s is the capture cross-section of recombination centre and N is the carrier concentration. As intense light falls on the sample, the lifetime decreases [30]. Stockman model explains the tendency of decrease in mobile charge carriers during the negative photoconductivity. According to this model, for the PMPIB crystal, the negative photoconductivity is based on the state between the Fermi level and the valance band [31]. This state has high capture cross sections for electrons and holes. Also this state can capture electrons from the conduction band and holes from the valance band. Thus the net number of mobile charge carriers is reduced due to incident radiation giving raise to negative photoconductivity [32].

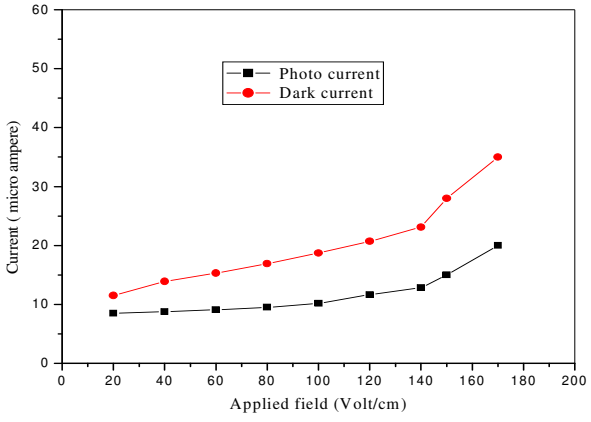

Figure-11
Field dependent photoconductivity of PMPIB single crystal

LDTA: Laser damage threshold of a material is defined as the maximum permissible optical power for a particular crystal to cause a breakdown of the material[33]. According to Nakatani et al[34], the multiple shot [n-on-1] damage threshold is the minimum power level below which the crystal does not suffer damage after multiple shot pulses. For crystals which are used in commercial frequency doublers, the multiple shot surface damage threshold is the most important parameter. In order to measure the laser damage threshold as grown crystals of PMPIB about 5mm in diameter and 3mm in thickness were placed in front of a Q-switched Nd:YAG laser through slit (area 0.3 mm^2) following a focusing lens. Based on the multishot method, the damage was found visually. After that the crystal was replaced by a power meter to measure the power density which was used to cause damage in the crystal. In the present work, laser damage was found to be 0.57 GW/cm^2 which is higher than that of KDP (0.2 GW/cm^2) as lower than that of urea (15 GW/cm^2). The high damage threshold reveals that the compound is chemically stable and neither hygroscopic nor soluble in water.

NLO report: A preliminary study on the SHG efficiency of the grown PMPIB crystal was measured by Powder Kurtz method. The measured SHG efficiency was compared with KDP and found that the grown PMPIB crystal has nearly 1.5 times higher NLO efficiency than KDP, which is familiar inorganic NLO material.

Second Harmonic Generation efficiency and Phase matching curve: The fundamental wavelength emitted from a Q-switched Nd:YAG laser was used. A photodiode was used as a reference to monitor the pulse fluctuations in the input beam. PMPIB sample was grinded using standard sieves in the range less than 106 µm to above 150 µm. The measurement of SHG output for various particle size show the increasing SHG intensities with increasing particle size upto 150 µm as shown in figure 12, which confirm the phase matching behavior of the material. Hence PMPIB crystal can be used as an efficient frequency doubler and optical parametric oscillator provided if large size single crystal are grown.

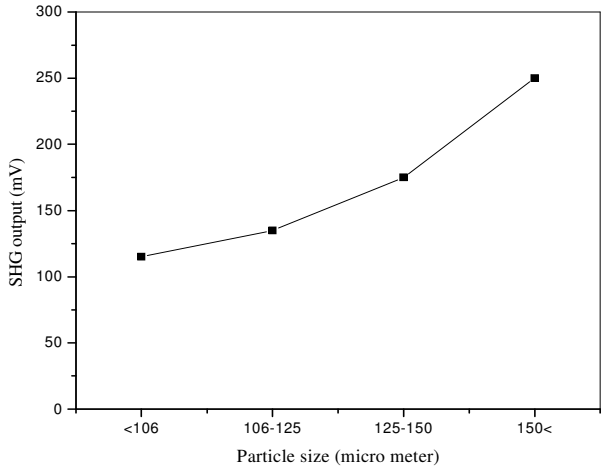

Figure-12
Phase matching curve of PMPIB single crystal

Conclusion

PMPIB single crystal was synthesized through solvent- free reaction mechanism and grown by both slow solvent evaporation technique and S-R method. The lattice parameters and the noncentrosymmetric space group were confirmed by single crystal XRD analysis. XRPD analysis ascertained the perfect crystalline arrangement in PMPIB structure. FTIR spectral analysis confirms the presence of functional groups and their mode of vibrations in PMPIB crystal. UV-Vis-NIR spectral analysis has reached the conclusion that PMPIB molecule exhibits orbital π- electron delocalization due to the mesomeric effect is responsible for its nonlinear optical response and absorption in near UV-region charge transfer transition which proves that PMPIB has a good NLO property. H1 and C13 NMR spectral analysis strongly confirm the carbon-hydrogen network among imino and methoxy functional groups. The existence of second harmonic generation (SHG) signal was observed by using ND: YAG laser with the fundamental wavelength of 1064 nm. The high damage threshold reveals that the compound is chemically stable and neither hygroscopic nor soluble in water and hence PMPIB can be used in frequency doubler system. The photoconductivity study of PMPIB revealed negative photoconductivity of the sample.

Acknowledgement

The authors would like to thank University Grants Commission, Bahadurshah Zafar Marg, New Delhi – 110 002, India for funding to this Major Research Project (File No.: 40-434/2011(SR), dt. 04.07.2011) and Dr. M. Basheer Ahamed, The Head, Department of Physics, Crescent Engineering College, Chennai-600 048, India for testing SHG, using Q-switched Nd:Yag laser.

References

1. Kitazawa M., Higuchi R.H., Takahasi M., Wada T. and Sasabe H., Ultraviolet generation at 266 nm in a novel organic nonlinear optical crystal: l-pyrrolidone-2-carboxylic acid, *Appl. Phys. Lett.,* **64,** 2477-2479 **(1994)**

2. Misoguti L., Verela A.T., Nunes F.D., Bagnato V.S., Melo F.E.A., Filho J.M. and Zilio S.C., Optical properties of L-alanine Organic Crystals, *Opt. Mater.*, **6(3),** 147-152 **(1996)**

3. Wang W.S., Aggarwal M.D., Choi J., Bhat K., Gebre T., Shields A.D., Penn B.G. and Frazier D.O., Solvent effects and polymorphic transformation of organic nonlinear optical crystal L-pyroglutamic acid in solution growth processes: I. Solvent effects and growth morphology, *J. Cryst Growth*, **198-199,** 578-582 **(1999)**

4. Siltvast W.T., *Laser Fundamentals*, (2nd Edn.) Cambridger University Press **(2004)**

5. Lal R.B., Zhang H.W., Wang W.S., Aggarwal M.D., Howard W.H. Lee and Penn B.G., Crystal growth and optical properties of 4-aminobenzophenone crystals for NLO applications, *J. Cryst Growth*, **174,** 393-397 **(1997)**

6. Periyasamy B.K., Jebes R.S., Gopalakrishnan N. and Balasubramaniam T., Development of NLO tunable band gap organic devices for optoelectronic applications, *Mater. Lett.*, **61(21),** 4246-4249 **(2007)**

7. Ravindra H.J., Harrison W.T.A., Suresh Kumar M.R. and Dharmaprakash S.M., Synthesis, crystal growth, characterization and structure–NLO property relationship in 1,3-bis (4-methoxyphenyl) prop-2-en-1-one single crystal, *J. Cryst. Growth*, **311(2),** 310-315 **(2009)**

8. Plagvet A., Guillaume M., Champagne B., Rougier L., Mancois F., Rodriguez V., Pozzo J.L., Ducasse L. and Castet F., Investigation on the Second-Order Nonlinear Optical Responses in the Keto-Enol Equilibrium of Anil Derivatives, *J. Physical Chemistry C,* **112,** 5638-5645 **(2008)**

9. Volodymyr V. Nesterov, Mikhail Yu, Antipin and Vladimir N. Nesterov: Thermally Stable Imines as New Potential Nonlinear Optical Materials, *Cryst. Growth and Design,* **4 (3),** 521-531 **(2004)**

10. Begland R.W., Hartter D.R., Jones F.N., Sam D.J., Sheppard W.A., Webster O.W. and Weigert F.J., Hydrogen cyanide chemistry, VIII. New chemistry of diaminomaleonitrile, Heterocyclic synthesis, *J. Org. Chem.*, **39 (16),** 2341-2350 **(1974)**

11. Ohtsuka Y., Chemistry of diaminomaleonitrile, II, Preparation of the open-chain adduct with ketone in phosphorus pentoxide-ethanol system, *J. Org. Chem.,* **41(4),** 629-683 **(1976)**

12. Ohtsuka Y., Chemistry of diaminomaleonitrile, Reaction with isocyanate: a novel pyrimidine synthesis, *J. Org. Chem.*, **43(16),** 3231-3234 **(1978)**

13. Ohtsuka Y., Chemistry of diaminomaleonitrile, Nitrile hydration of the Schiff bases, *J. Org. Chem.,* **44 (5),** 827-830 **(1979)**

14. Wöhrle D., Bohlen H. and Rothkopf H.W., Polymeric Schiff base chelates and their precursors, Synthesis of Schiff base chelates from diaminomaleonitrile and fundamental investigation of their activity for the valence isomerisation of quadricyclane to norbornadiene, *Makromol. Chem.*, **184**, 763-778 **(1983)**

15. Wang Y., Yu Z., Sun Y., Yishi Wang and Lu L., Synthesis, vibrational spectral and nonlinear optical studies of N-(4-hydroxy-phenyl)-2-hydroxybenzaldehyde-imine: A combined experimental and theoretical investigation, *Spectrochimica Acta Part A; Molecular and Biomolecular spectroscopy,* **79(5)**, 1475-1482 **(2011)**

16. Mukesh M.J. and Bharat B.B., Crystal structure optimization, Semi-empirical quantum chemical calculations and Non-linear optical property of a thiazolo [3, 2-a] pyrimidine derivative, *Res. J. Recent Sci.,* **1(ISC-2011),** 337-340 **(2012)**

17. Volodymr V.N., Mikhail Y.A., Vladimir N.N., Craig E.M., Beatriz H.C. and Tatiana V.T., Thermally stable heterocyclic imines as new potential nonlinear optical materials, *J. Phys. Chem. B,* **108***,* 8531-8539 **(2004)**

18. Rashidi N.A. and Berad B.N., Synthesis, characterization and de-tert-butylation of 4-N-t-butyl-5-aryl imino-1,2,4 triazolidine-3-thiones into 5-arylimino-1,2,4 triazolidine-3-thiones, *Res. J. Recent Sci.,* **1(ISC-2011),** 79-84 **(2012)**

19. Prajapati Ajaypal, Synthesis, Antimicrobial and Insecticidal Activity Studies of 5-Nitro N'-[Arylidenhydrazidomethyl Indole] 2-(Substituted Aryl)-3-(N'-Indolyl Acetamiddyl)-4-Oxothiazolidines, *Res. J. Recent Sci.,* **1(ISC-2011),** 99-104 **(2012)**

20. Prabhakar Y., Prasad K.R.S. and Kumar J.V.S., Microwave assisted synthesis of 3-(4-Ethylbenzyl)-1(4methoxybenzyl)-6-(methylthio)-1, 3, 5-triazine-2, 4 (1H, 3H)-dione derivatives Under solvent free condition with high yields, *Res. J. Recent Sci.,* **1(ISC-2011),** 105-109 **(2012)**

21. Girgaonkar M.V. and Shirodkar S.G., Synthesis, characterization and Biological studies of Cu(II) and Ni(II) complexes with New Bidentate Shiff's base ligands as 4-hydroxy-3-(1-(arylimino)ethyl)chromen-2-one, *Res. J. Recent Sci.,* **1 (ISC-2011),** 110-116 **(2012)**

22. Hisatake K., Tanka S. and Yovko A., Evaporation rate of water in a vessel, *J. Appl. Phys.,* 1993**, 73***,* 7395 – 7401 **(1993)**

23. Pavia D.L., Lampman G.M., Kriz G.S. and Vyvyan J.A., *Introduction to Spectroscopy,* 4th Edn., Brookescole Publishers, California **(2008)**

24. Banwell C.N. and McCASH E.M., *Fundamentals of Molecular Spectroscopy, 4th Edn.* Mc-Graw-Hill **(1994)**

25. Ushasree P.M., Jayavel R. and Ramasamy P., Growth and characterisation of phosphate mixed ZTS single crystals, *Mater. Sci. Eng. B,* **65(3),** 153-158 **(1999)**

26. Charles Kittel, *Introduction to Solid State Physics, 7th Edn.,* John Wiley & Sons, Singapore, **(2007)**

27. Ganesh R.B., Kanna V., Sathyalakshmi R. and Ramasamy P., The growth of l-Glutamic acid hydrochloride crystals by Sankaranarayanan–Ramasamy (SR) method, *Mater. Lett.,* **61(3),** 706-708 **(2007)**

28. Hundelshausen U.V., The growth of l-Glutamic acid hydrochloride crystals by Sankaranarayanan–Ramasamy (SR) method, *Phys. Lett. A,* **34(7),** 405-406 **(1971)**

29. Bube R.H., *Photoconductivity of Solids*, Wiley, New York **(1981)**

30. Ashraf I.M., Elshaik H.A. and Badr A.M., Photoconductivity in Tl4S3 layered single crystals, *Cryst. Res. Technol.*, **39(1)***,* 63-70 **(2004)**

31. Pandi S. and Jayaraman D., Studies on photoconductivity of C60 and C60-doped poly(vinylchloride), *Mater. Chem. Phys.,* **71(3)**, 314-317 **(2001)**

32. Joshi V.N., *Photoconductivity,* Marcel Dekker, New York, **(1990)**

33. Dhanuskodi S., Jeyakumari A.P., Manivannan S., Philip J. and Tiwari S.K., Semiorganic nonlinear optical material for frequency doubling: Preparation and properties of sodium p-nitrophenolate dihydrate (SPNP), *Spectrochimica Acta Part A,* **66(2),** 318-322 **(2007)**

34. Nakatani H., Bosenberg W.R., Cheng L.K. and Tang C.L., Laser-induced damage in beta-barium metaborate, *Appl. Phys. Lett.,* **53**, 2587-2589 **(1978)**